Rapid Plasma Membrane Anchoring of Newly Synthesized p59^{fyn}: Selective Requirement for NH_2-Terminal Myristoylation and Palmitoylation at Cysteine-3

Wouter van 't Hof and Marilyn D. Resh

Cell Biology and Genetics Program, Sloan-Kettering Institute for Cancer Research, New York, 10021

Abstract. The trafficking of Src family proteins after biosynthesis is poorly defined. Here we studied the role of dual fatty acylation with myristate and palmitate in biosynthetic transport of p59^{fyn}. Metabolic labeling of transfected COS or NIH 3T3 cells with [^{35}S]methionine followed by analysis of cytosolic and total membrane fractions showed that Fyn became membrane bound within 5 min after biosynthesis. Newly synthesized Src, however, accumulated in the membranes between 20–60 min. Northern blotting detected Fyn mRNA specifically in soluble polyribosomes and soluble Fyn protein was only detected shortly (1–2 min) after radiolabeling. Use of chimeric Fyn and Src constructs showed that rapid membrane targeting was mediated by the myristoylated NH_2-terminal sequence of Fyn and that a cysteine at position 3, but not 6, was essential. Examination of $G\alpha_o$-, $G\alpha_s$-, or GAP43-Fyn fusion constructs indicated that rapid membrane anchoring is exclusively conferred by the combination of N-myristoylation plus palmitoylation of cysteine-3. Density gradient analysis colocalized newly synthesized Fyn with plasma membranes. Interestingly, a 10–20-min lag phase was observed between plasma membrane binding and the acquisition of non-ionic detergent insolubility. We propose a model in which synthesis and myristoylation of Fyn occurs on soluble ribosomes, followed by rapid palmitoylation and plasma membrane anchoring, and a slower partitioning into detergent-insoluble membrane subdomains. These results serve to define a novel trafficking pathway for Src family proteins that are regulated by dual fatty acylation.

In fundamental cell biological processes such as signal transduction at the plasma membrane or intracellular membrane fusions during vesicular transport, cytoplasmic proteins are recruited to and released from the cytoplasmic surface of cellular membranes (6, 44). In order to perform their functions at the correct time and place, these cytoplasmic proteins must rely on regulated processes guiding their binding to the cytoplasmic leaflet of the membrane lipid bilayer (6, 19, 40, 41). In recent years, modification with lipophilic moieties has been described as an important mechanism involved in membrane anchoring of cytoplasmic proteins. Two main types of protein acylation have been observed in eukaryotic cells: fatty acylation with myristate and palmitate and isoprenoylation with farnesyl or geranylgeranyl moieties (6, 19, 20, 40, 56).

Please address all correspondence to M.D. Resh, Cell Biology and Genetics Program, Sloan-Kettering Institute for Cancer Research, 1275 York Avenue, Box 143, New York, NY 10021. Tel.: (212) 639-2514. Fax: (212) 717-3317. E-Mail: m-resh@ski.mskcc.org

Many acylated proteins contain a combination of two membrane anchoring features (40, 41). This "two-signal mode" for membrane anchoring (40, 41) is highlighted by proteins belonging to the Src family and α subunits of heterotrimeric G–protein complexes, which are modified at their NH_2-termini with both myristate and palmitate (40). Proteins belonging to the Ras and Rab families carry the combination of isoprenyl groups and palmitate at their COOH-termini (16, 41). In addition, for Src, HIV-Gag-1 and the MARCKS protein, N-myristoylation has been observed in combination with NH_2-terminal clusters of basic amino acids (32, 49, 50, 57). These basic motifs have been reported to direct membrane association by interaction with negatively charged phospholipids enriched in the cytoplasmic leaflet of cellular membranes (reviewed in [39]). Interestingly, a similar combination, consisting of farnesylation plus a basic amino acid motif, has been observed at the COOH terminus of the K-Ras4B isoform (31), showing that the two signal combinations are conserved and can act at either the NH_2- and the COOH-termini of proteins (40, 41).

Members of the Src family of nonreceptor tyrosine kinases all share extensive sequence homology with the proto-oncogene pp60^{src}. The nine members Src, Yes, Lck,

Fyn, Lyn, Yrk, Blk, Hck, and Fgr contain four regions of sequence similarity, called Src Homology (SH)[1] domains. These include the COOH-terminal tyrosine kinase (SH1) and the internal SH2 and SH3 domains. The fourth consensus sequence, SH4, is located on the NH_2 terminus and carries the signals involved in the attachment of the fatty acids myristate and palmitate (40). The covalent attachment of myristate to an NH_2-terminal glycine occurs cotranslationally (54) and is mediated by the soluble enzyme N-myristoyl transferase (NMT) (20, 51). Recently, it was shown that several Src family members are also modified with palmitate (1, 34, 48) and that dual fatty acylation with myristate and palmitate regulates their membrane binding and subcellular distribution (1, 42, 43).

Currently, the molecular mechanism for trafficking of dually acylated Src family proteins from their site of synthesis to the membrane, remains poorly defined. Using $p59^{fyn}$ (1) as a model, we have studied the role of N-myristoylation plus palmitoylation in the trafficking Src family proteins after biosynthesis. We observed that newly synthesized Fyn became rapidly bound to the plasma membrane, within 5 min after biosynthesis, whereas newly synthesized v-Src required 20–60 min to accumulate in the membrane fraction. Northern blotting confirmed that Fyn is initially synthesized on soluble ribosomes in the cytoplasm. Experiments with mutant or chimeric Fyn constructs indicated that the rapid membrane targeting of biosynthetic Fyn is directed by its NH_2-terminal sequence. Subsequent mutational analysis showed that the rapid membrane binding phenotype of newly synthesized Fyn is encoded exclusively by the combination of N-myristoylation and palmitoylation at cysteine-3. In labeling experiments that were combined with extraction with the nonionic detergent Triton X-100, a significant lag-phase was observed between membrane binding and the acquisition of complete detergent insolubility of biosynthetic Fyn, indicating that dual acylation of Fyn is not a direct targeting signal for association with detergent resistant plasma membrane complexes. We present a model for the biosynthetic pathway for Fyn, in which cotranslational N-myristoylation on soluble ribosomes is rapidly followed by palmitoylation at cysteine-3 and plasma membrane anchoring, followed by association of Fyn with the detergent resistant matrix.

Materials and Methods

Materials

Cell culture reagents and RNA molecular weight markers were purchased from Gibco Laboratories (Grand Island, NY). cDNAs for human Fyn, c-Src, or v-Src in pCMV-5 (1) and p65-VALO (37), containing full-length β-galactosidase from *E. coli* were used from lab stocks. Human TGF-β I Receptor cDNA (14), modified with an HA tag and subcloned into pCMV-5 (53) and rabbit polyclonal antiserum against human TGF-β I Receptor were kindly provided by Drs. Joan Massagué and Frances Weis-Garcia (Sloan-Kettering Institute, New York). [^{35}S]Methionine (Tran^{35}S-label), 9,10-[^{3}H]myristate, 9,10-[^{3}H]palmitate, [^{125}I]Na-I and [α-^{32}P]dCTP were purchased from DuPont New England Nuclear (Boston, MA). Synthesis and radioiodination of IC-16 and IC-13 fatty acid analogues were performed as previously described (4). Rabbit polyclonal antisera raised against Fyn SH43 protein, containing amino acids 1-148 of Fyn (4), or v-Src were from lab stocks. Rabbit anti–β-galactosidase polyclonal antiserum was from Promega (Madison, WI) and protein A–agarose was from Santa Cruz (Palo Alto, CA). 4-Methylumbelliferone substrates were from Sigma Chem. Co. (St. Louis. MO) and OptiPrep™ was purchased from Nycomed Pharma (Oslo, Norway).

Construction of Fyn Chimeras ($G\alpha_o$(10)-Fyn, $G\alpha_s$(10)-Fyn, and GAP43(10)-Fyn

Chimeric cDNAs in which the first 10 amino acids of Fyn were replaced by the corresponding sequences of $G\alpha_o$, $G\alpha_s$ (23), or GAP43 (22) were generated by PCR using the following procedure. Sense oligonucleotides were synthesized to encode the upstream region of pGEM3Z, followed by the first 10 amino acids of human $G\alpha_o$ or $G\alpha_s$ and amino acids 11-15 of human Fyn. For the GAP43 construct a sense oligonucleotide was synthesized to encode a BamHI site, the upstream region of pGEM3Z, the first 10 amino acids of human GAP43 and amino acids 11-15 of human Fyn. An antisense oligonucleotide was used corresponding to a region of the SH3 domain of Fyn (1). These primers were used with pGEM3Z-Fyn as a template to generate chimeric cDNAs by PCR. The PCR products obtained using the $G\alpha_o$ or $G\alpha_s$ sense primers were digested with NcoI and BstXI to generate 76 basepair fragments that were used to replace the corresponding fragments of Fyn in pSP65. The PCR product obtained using the GAP43 sense primer was digested with BamHI and BstXI to generate a 100-bp fragment that was used to replace the corresponding fragment of Fyn in pSP65. The constructs were subsequently digested with EcoRI and SalI, followed by ligation of $G\alpha_o$(10)-Fyn, $G\alpha_s$(10)-Fyn, or GAP43(10)-Fyn chimeric cDNA into EcoRI and SalI cut pCMV5. All constructs were verified by DNA sequencing before use in transfection studies.

Cell Culture, Transfection, and Metabolic Labeling

COS-1 cells (ATCC) were grown in DMEM, supplemented with 10% FBS (Gemini Bioproducts), penicillin (50 U/ml), and streptomycin (50 μg/ml). Stable clones of NIH-3T3 cells expressing human wt Fyn were grown in DMEM, supplemented with 10% calf serum, penicillin (50 U/ml), and streptomycin (50 μg/ml). Cells were cultured in an atmosphere of 5% CO_2 at 37°C and were passaged every 2–3 d. COS-1 cells were transfected according to the DEAE-dextran method as follows. Semi-confluent monolayers on 100-mm plastic tissue culture dishes were incubated for 2.5 h at 37°C with DMEM containing 10% Nu Serum (Collaborative Research Labs, Bedford, MA), 100 μM chloroquine, 400 μg/ml DEAE-dextran, and 5–10 μg DNA. Cells were incubated for 1 min in PBS containing 10% DMSO, washed with DMEM, and incubated overnight in DMEM containing 10% FBS. The next day, cells were trypsinized and experiments were performed the following day (2 d after transfection). Transfected cells were metabolically radiolabeled at 37°C with 100 or 500 μCi/ml [^{35}S]methionine, after starvation for 1 h at 37°C in DMEM minus methionine, containing 2% dialyzed FBS. For radiolabeling with fatty acids, cells were starved for 1 h at 37°C in DMEM containing 2% dialyzed FBS, followed by incubation with either 20 μCi/ml [^{3}H]myristate or 100 μCi/ml [^{3}H]palmitate at 37°C. Alternatively, 10–20 μCi/ml [^{125}I]IC-13 or [^{125}I]IC-16 were used (1, 36). Labeling experiments up to 20 min were performed in a waterbath at 37°C in media supplemented with 50 mM Hepes, pH 7.4. Radiolabeling for longer times was performed in a tissue culture incubator with pre-equilibrated medium.

Extraction of Transfected Cells with Non-ionic Detergent

Radiolabeled COS-1 or NIH-3T3 cells were extracted with a 1% Triton X-100 solution as previously described (17). Cells on 60-mm dishes were rinsed with ice-cold STE (50 mM Tris/HCl, pH 7.4, 150 mM NaCl, 1 mM EDTA) and incubated for 5 min at 4°C with 0.8-ml Csk buffer (10 mM Pipes pH 6.8, 100 mM KCl, 2.5 mM $MgCl_2$, 1 mM $CaCl_2$, 300 mM sucrose, and 1% Triton X-100) containing protease inhibitors (1 mM PMSF, 10 μg/ml leupeptin, and 10 μg/ml aprotinin), followed by 0.2 ml fresh buffer for 1 min. The two detergent washes, containing detergent soluble (S) material, were pooled and 0.25 ml 5× lysis buffer was added. The remaining fraction on the dishes, containing detergent resistant (R) material, was subsequently scraped from the plate in 1 ml 1× lysis buffer (50 mM Tris, pH 8.0, 150 mM

1. *Abbreviations used in this paper*: IC-13, 13-[^{125}I] iodotridecanoic acid; IC-16, 16-[^{125}I] iodohexadecanoic acid; NMT, N-myristoyl acyltransferase; PAT, palmitoyl acyltransferase; SH, Src Homology domain; TBR-I, transforming growth factor β type-I receptor.

NaCl, 2 mM EDTA, 1% NP-40, 0.5% deoxycholate, 5 mM NaF). Both fractions were clarified for 15 min at 100,000 *g* and analyzed by immunoprecipitation and SDS-PAGE as described below.

Subcellular Fractionation and Marker Enzyme Analysis

Analysis of Cytosol (S100) and Total Membranes (P100). Radiolabeled cells were washed and scraped from the dishes in ice-cold STE. Cells were spun for 5 min at 1,500 rpm in a refrigerated tabletop centrifuge, resuspended in hypotonic buffer (10 mM Tris/HCl pH 7.2, 0.2 mM $MgCl_2$, 100 mM Na_3VO_4) supplemented with protease inhibitors, and incubated on ice for 10 min, followed by homogenization with 25 strokes in a 1.5-ml Dounce homogenizer with a tight pestle. The homogenate was adjusted to 250 mM sucrose and 1 mM EDTA and centrifuged for 45 min at 100,000 *g* (50,000 rpm in TLA 100.2 or 100.3 rotor) in an Optima TL Ultracentrifuge (Beckman Instrs., Fullerton, CA). The pellet (P100), containing total cellular membranes, was resuspended in lysis buffer supplemented with protease inhibitors and the soluble fraction (S100) was supplemented with 0.2 vol of 5× concentrated lysis buffer. Samples were lysed for 15 min on ice, clarified by centrifugation for 15 min at 100,000 *g* and immunoprecipitated. Antibody titration experiments were performed to verify that immunoprecipitation reactions occurred under conditions of antibody excess, allowing for quantitative recovery of Fyn and Src from P100 and S100 fractions.

Analysis of Linear Density Gradients. The following modifications were made for analysis of the intracellular distribution of biosynthetic Fyn. Only stably transfected NIH-3T3 cells were used for linear density gradient analysis. All steps were performed with an isotonic homogenization buffer (0.25 M Sucrose, 20 mM Hepes, pH 7.4, 1 mM EDTA), containing protease inhibitors. For each individual gradient, cells from six sub-confluent 100-mm plastic dishes were used equivalent to roughly 10 mg cellular protein. Cells were scraped, spun down for 5 min at 1,500 rpm, resuspended in 1 ml isotonic homogenization buffer with protease inhibitors, and homogenized with 15 strokes in a 1.5-ml Dounce homogenizer with a tight pestle. Nuclei and unbroken cells were removed by centrifugation for 10 min at 500 *g*. The Dounce homogenizer was rinsed with 0.2 ml homogenization buffer and this solution was used to resuspend the nuclear pellet, followed by a respin for 10 min at 500 *g*. Subsequently, the combined postnuclear supernatants (PNS) were centrifuged for 45 min at 100,000 *g*, and the resulting P100 fraction was resuspended in 1 ml isotonic homogenization buffer with protease inhibitors by five strokes in the Dounce homogenizer and layered on top of continuous iodixanol density gradients (25.0–2.5% wt/vol OptiPrep™, from stock solution diluted in 0.25 M sucrose/TE). Gradients were centrifuged for 3 h at 100,000 *g* (38K in SW40Ti rotor) and fractionated into ~0.7 ml samples, starting from the bottom of the gradient. For analysis of marker enzyme activities, 20–50-μl samples were taken from each fraction. Assays, routinely performed in duplicates in 96-well microtiter plates (Costar, Boston, MA), were started by adding 200 μl enzyme assay mixed to each sample. α-Glucosidase II activity was assayed in 150 mM Citrate/phosphate pH 6.5, 1 mM 4-Methylumbelliferone-α-D-glucoside, α-Mannosidase II in 150 mM phosphate buffer, pH 6.0, containing 0.02% Triton X-100, 1 mM 4-Methylumbelliferone-α-D-mannopyranoside, and alkaline phosphatase activity was measured in 100 mM Tris/NaOH pH 9.5, 100 mM NaCl, 5 mM $MgCl_2$, 1 mM 4-Methylumbelliferone-phosphate. Reactions were allowed to proceed for 2–4 h at 37°C and stopped by addition of 100 μl ice-cold 1 M Glycine/NaOH, pH 10, 1 M Na_2CO_3. Fluorescence was measured at λ_{ex} 360 nm, λ_{em} 460 nm using a CytoFluor™ 2350 Fluorescence measurement system (Millipore, Bedford, MA).

Immunoprecipitation, Gel Electrophoresis, and Quantitation

To each clarified sample in lysis buffer either 2 μl anti-Fyn, 2 μl anti-Src, 1 μl anti-TBR I, or 1 μl anti-β-Gal rabbit polyclonal antiserum was added. After addition of 10 μl protein A–agarose solution, samples were incubated for 2–12 h at 4°C. Immunoprecipitates were washed twice with lysis buffer and once with TE (10 mM Tris/HCl, pH 7.2, 1 mM EDTA) and analyzed by SDS-PAGE. Radiolabeled proteins were visualized by exposure to X-omat or BioMax film (Eastman Kodak, Rochester, NY) and quantified by cutting out gel slices, followed by liquid scintillation counting in EcoLume (ICN, Costa Mesa, CA). Alternatively, gels were exposed to phosphorimager screens and quantitation was performed using the ImageQuant software provided with the phosphorimager system (Molecular Dynamics, Sunnyvale, CA).

Analysis of Soluble and Membrane-bound Polyribosomes

All steps were performed at 4°C under RNAse-free conditions and all solutions, buffered with Hepes instead of Tris, were pretreated with 0.2% DEPC and supplemented with 5 mM DTT and 0.5 U/ml rRNAsin (New England Biolabs, Beverly, MA).

Flotation Assay for Membrane-bound Polysomes. The protocol was adapted from the nascent chain targeting assay by Lauring et al. (24). Homogenization of transfected cells was performed with hypotonic buffer, containing 10 mM Hepes/KOH, pH 7.4. Postnuclear supernatants were adjusted to 50 mM Hepes/KOH, pH 7.4, 50 mM KOAc, and 5 mM $Mg(OAc)_2$ (HKM buffer), layered on top of a 2-ml cushion of 1 M sucrose/HKM, and centrifuged for 2 h at 200,000 *g* in an SW 55Ti rotor (46,000 rpm). The supernatant and sucrose cushion were discarded and the polyribosomal pellet was carefully resuspended in 1 ml 2.1 M sucrose/HKM. Subsequently, a discontinuous sucrose gradient was generated by overlayering with 3 ml of 1.9 M sucrose/HKM and 1 ml HKM, respectively. After a centrifugation step for 2 h, at 200,000 *g*, membrane-bound (Mb) ribosomes were collected from the 1.9-M sucrose, HKM interface, whereas soluble (S) polysomes were collected from the 2.1 M sucrose cushion. Membrane and soluble polysomal samples were diluted in 5 vol of HKM, and polyribosomes were precipitated by centrifugation for 2 h at 200,000 *g*.

RNA Extraction and Northern Blotting Analysis. Membrane-bound and soluble polyribosomes were resuspended in 1 ml Ultraspec RNA solution (Biotecx, Houston, TX) and incubated for 10 min at 4°C. After addition of 200 μl chloroform and centrifugation for 10 min in an Eppendorf centrifuge, the clear upper-phases containing the RNA were collected, supplemented with equal volumes of 2-propanol, and incubated for 10 min at 4°C. After centrifugation for 15 min at top speed in an Eppendorf centrifuge, RNA pellets were washed with 80% ethanol in TE, air-dried for 2–3 min under vacuum and redissolved in 10 μl TE. Routinely, 1 μl was tested for rRNA intactness on a 1% agarose gel and the remainder was resolved on a 1% formaldehyde-agarose gel, followed by transfer to GeneScreen Plus hybridization transfer membranes (DuPont NEN) and UV-crosslinking of RNA to the membranes using a Stratalinker (Stratagene, La Jolla, CA). Fyn, v-Src, or TBR-I RNA species on hybridization membranes were detected with random-primed (Stratagene) ^{32}P-labeled fragments that were synthesized using the following DNA templates. A specific template for Fyn, an 0.7-kB cDNA fragment encoding the NH_2-terminal Fyn sequence, was obtained by gel purification after SmaI digestion of pSP65-Fyn (1). For v-src, a 1.9-kB fragment encoding the entire gene, was obtained after NcoI and BglII digestion of pGEM3z-v-src (1). An 0.8-kB template for TBR-I, encoding its unique NH_2-terminal ectodomain (14), was prepared by HindIII and XbaI digestion of pCMV5-TBR I-HA, followed by gel purification. Blots were first incubated for 1 h at 42°C with hybridization solution (5× SSPE, 5× Denhardt solution, 50% formamide, 1% SDS, 10% dextran sulphate, and 100 μg/ml denatured salmon sperm DNA), then overnight at 42°C with 0.5×10^6 cpm/ml denatured random probes in fresh hybridization buffer without salmon sperm DNA. The blots were washed twice for 15 min at RT with 1.0× SSPE/0.1% SDS and once with 0.2× SSPE/0.1% SDS for 15 min at 50°C before exposure to X-ray film or phosphorimager screens. For reprobing, blots were stripped by washing twice for 30 min at 80°C in 0.05× SSPE, 0.01 M EDTA, and 0.1% SDS, rinsed with 0.01× SSPE for 15 min at RT and hybridized as before.

Results

Newly Synthesized Fyn Is Rapidly Directed to Membrane Fractions

The subcellular distribution of newly synthesized Fyn and Src was studied by fractionation of pulse radiolabeled cells into cytosolic (S100) and total membrane (P100) fractions. COS-1 cells, transfected with wt Fyn or v-Src were radiolabeled for 5, 10 or 20 min at 37°C with [^{35}S]methionine, followed by homogenization and centrifugation at 100,000 *g*. Analysis of S100 and P100 fractions by immunoprecipitation (Fig. 1) revealed that newly synthesized Fyn was predominantly (>85%) in the membrane fractions after 5, 10 and 20 min of radiolabeling (Fig. 2 *A*). At these time-

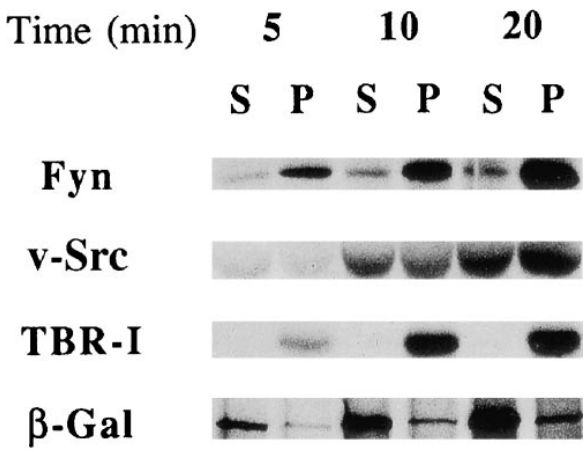

Figure 1. Subcellular distribution of newly synthesized Fyn and marker proteins in COS-1 cells. COS-1 cells were transfected with cDNAs encoding wild-type Fyn, v-Src, TBR-I, or β-galactosidase as described under Materials and Methods. Transfected cells on 60-mm plastic dishes were radiolabeled with 100 μCi/ml [^{35}S]methionine for 5, 10, or 20 min at 37°C, followed by homogenization and fractionation into a cytosolic (S100) and a total cellular membrane (P100) fraction, by centrifugation for 45 min at 100,000 *g*. The subcellular distribution of Fyn and marker proteins between the soluble and membrane fractions was analyzed by immunoprecipitation, followed by SDS-PAGE and autoradiography. Gels were exposed to film for 8–16 h.

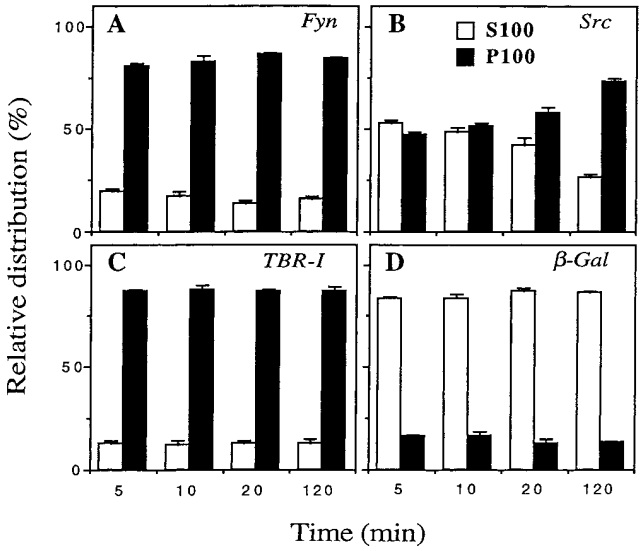

Figure 2. Quantitation of the subcellular distribution of newly synthesized Fyn. Cells were transfected, radiolabeled for the indicated amounts of time, homogenized and fractionated as described in the legend to Fig. 1. After detection of proteins by autoradiography, the radiolabeled bands were excised and quantified by liquid-scintillation counting. Total cpm after 5, 10, 20, and 120 min of labeling were Fyn (*A*) 642, 1699, 3542, and 28209 cpm, respectively; Src (*B*) 542, 1400, 2244, and 16223 cpm; TBR-I (*C*), 964, 2481, 3397, and 10668; β-galactosidase (*D*), 318, 922, 1894, and 13569. These numbers for total label incorporation represent the mean of three independent experiments, with individual measurements ranging within 20% of the mean. Blanks, measured by excising gel-slices in control lanes, contained 71 ± 3 cpm (n = 16).

points, significant amounts (~55%) of newly synthesized v-Src were still observed in the soluble fractions, followed by accumulation in the membrane fraction after radiolabeling for 120 min (Fig. 2 *B*). Identical results were obtained using constructs encoding c-Src instead of v-Src in COS-1 cells (not shown). As controls, COS-1 cells were transfected with transforming growth factor β type-I receptor (TBR-I), a transmembrane protein, and β-Galactosidase (β-Gal), a soluble protein. TBR-I was consistently present in the P100 fractions (Figs. 1 and 2 *C*), and β-Gal was primarily recovered from the S100 fractions (Figs. 1 and 2 *D*), confirming the identity of the cytosolic and total membrane fractions.

Control experiments were performed to verify that accumulation of biosynthetic Fyn and Src in the P100 fractions was caused by binding to membranes, rather than aggregation of overexpressed protein into insoluble complexes. P100 fractions from cells radiolabeled with [^{35}S]methionine for 5 min were resuspended, layered on 50% (wt/wt) sucrose cushions, and centrifuged for 1 h at 100,000 *g*. During centrifugation, membrane-bound material accumulates on top of the high density sucrose solutions, due to the buoyant density of membrane lipids, whereas insoluble material migrates through the sucrose cushion and pellets on the bottom of the tube. After centrifugation, samples were collected from the top of the 50% sucrose cushion and the pellet, and analyzed by immunoprecipitation. In two experiments, 86 ± 4% of radiolabeled Fyn and 96 ± 4% Src was recovered from the top of the 50% sucrose cushion, confirming the membrane-bound nature of newly synthesized Fyn and Src in the P100 fractions (Figs. 1 and 2).

Fyn Is Synthesized on Free Polyribosomes in the Cytoplasm

Most membrane proteins are synthesized on membrane-bound ribosomes, by virtue of an NH_2-terminal signal sequence that directs cotranslational anchoring to the ER membrane (52). Although Fyn has no apparent NH_2-terminal signal sequence for cotranslational membrane anchoring, the membrane binding behavior of the newly synthesized Fyn polypeptide is similar to that of transmembrane proteins (cf. Fig. 2, *A* and *C*). To determine the site of synthesis of Fyn protein, the localization of Fyn mRNA was assessed. The distribution of Fyn mRNA was compared to that of v-Src specific mRNA, which is known to be localized to free polyribosomes (25) and the mRNA specific for the type I transmembrane protein TBR-I (14), made on membrane-bound polysomes. COS-1 cells were cotransfected with cDNAs for Fyn, v-Src, and TBR-I, polyribosomes were isolated and fractionated into free and membrane-bound fractions (24), followed by mRNA isolation and separation on agarose/formaldehyde gels. After transfer to hybridization membranes, RNA species specific for Fyn, v-Src, and TBR-I were visualized and measured, using specific ^{32}P-labeled probes. For Fyn, a single RNA species of ~2.2 kB (Fig. 3 *A*) was found to be enriched in the soluble polyribosomal fraction (Fig. 3, *A* and *B*). The Fyn mRNA was of appropriate size (2) and its distribution was identical to that of v-Src mRNA, observed as a single spe-

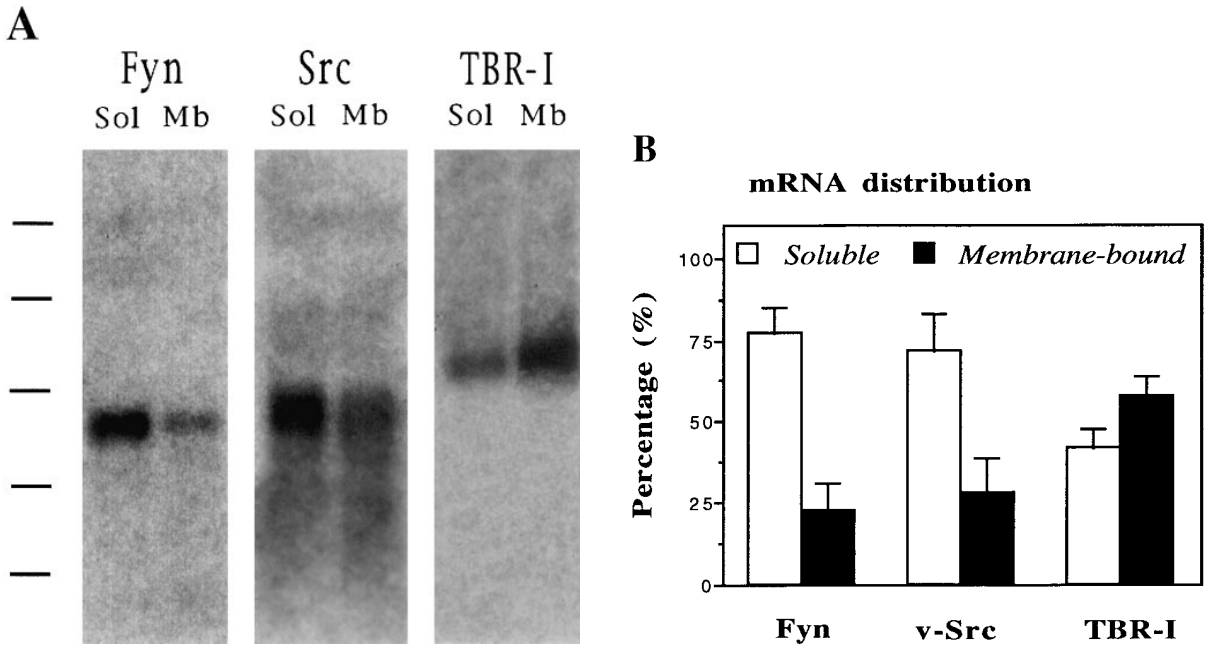

Figure 3. Northern blotting analysis of Fyn mRNA in soluble and membrane-bound polyribosomes. COS-1 cells were cotransfected with cDNAs for Fyn, Src, or TBR-I. Soluble and membrane-bound polyribosomal complexes were isolated as described under Materials and Methods. The detection of specific mRNA species in free or membrane-bound polyribosomal samples was performed by Northern blot analysis, using ^{32}P-labeled fragments specific for Fyn, v-Src, or TBR-I. (*A*) Distribution of Fyn, Src, or TBR-I specific mRNA in soluble (Sol) and membrane-bound ribosomes (Mb). From top to bottom, markers indicate the migration of RNA species of 7.5; 4.4; 2.4; 1.4; and 0.2 kB, respectively. Blots were exposed to film for 2–5 d. (*B*) Quantitation of the relative distribution of Fyn, Src, and TBR-I mRNA between soluble and membrane-bound ribosomes, measured by phosphorimager analysis. Values represent the mean of four independent experiments. Blots were exposed to phosphorimager screens for 12–36 h.

cies of ~2.4 kB (Fig. 3, *A* and *B*). In contrast, the majority of TBR-I specific mRNA (~3.0 kB; Fig. 3 *A*) was recovered from the membrane fraction (Fig. 3 *B*). No significant degradation for any of the mRNA species was observed (Fig. 3 *A*). Taken together, these results establish that Fyn is synthesized on soluble polyribosomes in the cytoplasm.

In the next experiment, the time scales of radiolabeling with [^{35}S]methionine were reduced in order to detect soluble Fyn precursors (Fig. 4). A significant amount (45%) of Fyn was detected in the S100 fraction after 1 min of radiolabeling at 37°C (Fig. 4 *A*). This soluble pool rapidly decreased to 35% and 25% after 2- and 4-min labeling, re-

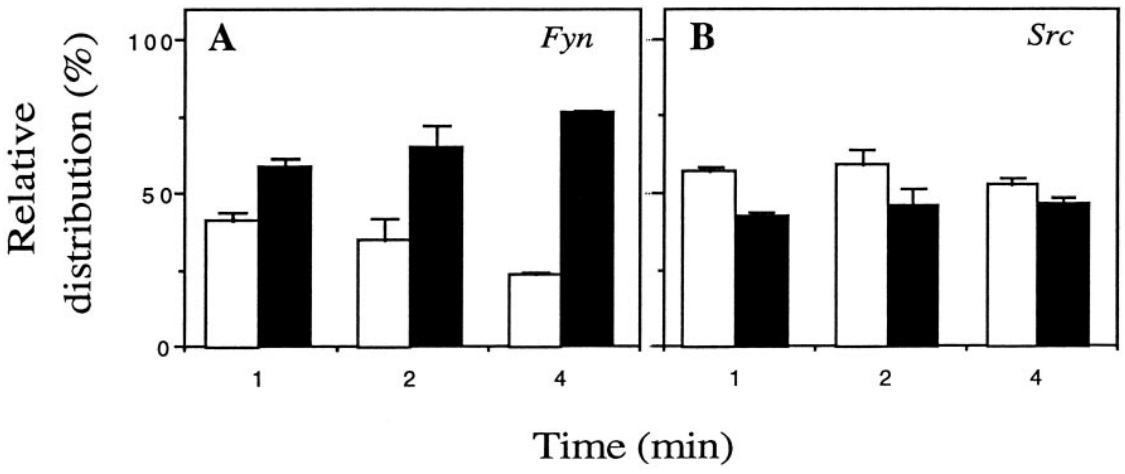

Figure 4. Subcellular distribution of newly synthesized Fyn, radiolabeled for 1, 2, and 4 min. COS-1 cells were transfected with Fyn or Src cDNA, homogenized, and fractionated as described in the legend to Fig. 1. Transfected cells on 100-mm plastic dishes were radiolabeled for 1, 2 or 4 min with 100 μCi/ml [^{35}S]methionine at 37°C and radiolabeled Fyn and Src were immunoprecipitated and applied to SDS-PAGE, followed by autoradiography and quantitation by liquid-scintillation counting. In two experiments, total counts for Fyn (*A*) were 456, 1035, and 2617 cpm, after 1, 2, and 4 min at 37°C, respectively. For Src (*B*) numbers were 237, 1357, and 2888 cpm, respectively. Blanks contained 72 ± 4 cpm (n = 4).

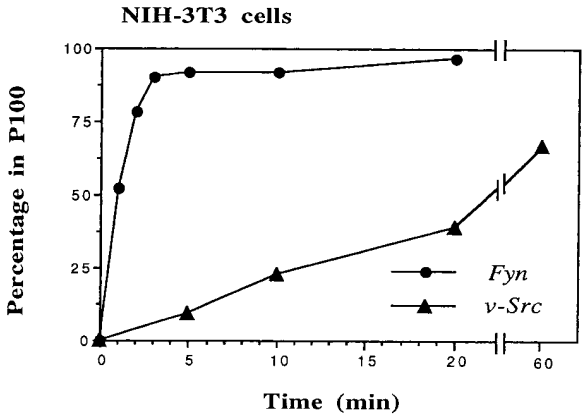

Figure 5. Membrane binding of newly synthesized Fyn and v-Src in stably transfected NIH-3T3 cells. NIH-3T3 cells stably expressing human Fyn or v-Src were radiolabeled for the indicated time intervals with 100 μCi/ml [^{35}S]methionine at 37°C. Cells were fractionated into S100 and P100 fractions as before and the distribution of Fyn and v-Src was analyzed by immunoprecipitation and SDS-PAGE, followed by quantitation by phosphorimaging after exposure for 7–14 d. In this figure and in the following figures, values represent the amount recovered in P100 fractions, as the percentage of total. These values are the mean of two or three experiments, with individual measurements ranging within 10% of the mean. Background values, measured in each individual lane containing radiolabeled protein, represented 20 ± 15% of total signal for Fyn (n = 12), and 10 ± 8% for v-Src (n = 8).

spectively, concomitant with a corresponding increase of radiolabeled Fyn in the P100 fractions (Fig. 4 *A*). In contrast, the distribution of v-Src after 1-, 2-, and 4-min labeling (Fig. 4 *B*) showed no significant changes compared to longer labeling times (Fig. 2 *B*). These observations indicate that immediately after biosynthesis (<1 min), Fyn exists as a soluble cytoplasmic protein, which subsequently becomes membrane bound between 2–4 min. Experiments to test for the accumulation of the soluble form of newly synthesized Fyn at lower temperatures (25°C, 20°C, or 15°C) or after energy (ATP) depletion, were unsuccessful because levels of radiolabel incorporation were limiting under these conditions (not shown).

Rapid Membrane Targeting of Newly Synthesized Fyn in Stably Transfected NIH-3T3 Cells

Since exogenous protein in transfected COS-1 cells can be overexpressed 20–50-fold above endogenous levels, it is possible that highly overexpressed protein may exhibit aberrant behavior. To test if the observed rapid membrane targeting of Fyn in COS-1 cells is a general phenomenon or an artifact driven by protein overexpression, we studied Fyn and v-Src in stably transfected NIH-3T3 cells, in which overexpression levels range from 5–10-fold. Confluent monolayers of Fyn or Src expressing 3T3 cell lines were radiolabeled with [^{35}S]methionine at 37°C and fractionated into S100 and P100 fractions as before. The distribution of Fyn and v-Src was analyzed by immunoprecipitation and SDS-PAGE, followed by quantitation through phosphorimaging. Expression levels in NIH-3T3 cells were confirmed to be much lower than in COS-1, as indicated by the longer exposure times to film and phosphorimager screens (see legends to Figs. 1 and 5). Analysis from three different experiments showed that in NIH-3T3 cells, newly synthesized Fyn was also rapidly targeted to the membrane fraction (Fig. 5). Initially, 1 min after biosynthesis, 50% of Fyn was soluble. Within 3 min, steady-state levels of membrane binding (90% in P100) were observed (Fig. 5). In contrast, analysis of v-Src in 3T3 fibroblasts shows that membrane-binding of v-Src was much slower (Fig. 5). Binding was linear for up to 20 min, and the steady state distribution (70% in P100) was only reached between 20 and 60 min. Interestingly, in experiments with 3T3 fibroblasts, the levels of Fyn in the S100 at steady state were lower (5–9%, Fig. 5) than those in COS-1 cells (15–25%, Fig. 2 *A*), indicating that overexpression of Fyn in COS-1 may lead to a slight buildup of Fyn in the cytosolic fraction. The experiments with 3T3 fibroblasts again serve to highlight the obvious difference between "rapid" membrane targeting of Fyn and the "slow" membrane binding of v-Src after biosynthesis.

Rapid Membrane Targeting of Fyn Depends on Myristoylation and a Cysteine at Position-3

Membrane binding of a variety of chimeric and mutant Fyn and v-Src constructs (1) (summarized in Table I) was monitored in order to unravel the mechanism behind the rapid biosynthetic membrane anchoring of Fyn. We focused on the NH_2-terminal SH4 region of Fyn which is known to contain the signals for membrane anchoring (1). Use of the Fyn(14)Src chimera, in which the first 14 amino acids of Fyn replaced those of v-Src (1), showed that these first 14 amino acids of Fyn were sufficient to induce rapid membrane targeting of v-Src, as illustrated by rapid accumulation of biosynthetic Fyn(14)Src in the P100 fractions (Fig. 6 *B*). Conversely, replacement of the first 14 amino acids of Fyn by the corresponding amino-terminal sequence of v-Src (Src(14)Fyn), resulted in slow membrane

Table I. Amino-Terminal Sequences of wt and Mutant Fyn and Src

	Amino acid position
	1 2 3 4 5 6 7 8 9 10
Fyn	Myr------- G C V Q C K D K E
G_2A-Fyn	A C V Q C K D K E
C_3S-Fyn	Myr------- G S V Q C K D K E
C_6S-Fyn	Myr------- G C V Q S K D K E
Src	Myr------- G S S K S K P K D
S_3C-Src	Myr------- G C S K S K P K D
S_6C-Src	Myr------- G S S K C K P K D
$G\alpha_o$	Myr------- G C T L S A E E R
$G\alpha_s$	M G C L G N S K T E
GAP-43	M L C C M R R T K Q

The sequences of the first ten amino acids of each Fyn construct are shown with mutant amino acids underlined. Point mutants were constructed by site-directed mutagenesis (1). The G_2A-Fyn mutant has glycine-2 replaced by alanine, resulting in loss of myristoylation (1). C_3-S-Fyn and C_6S-Fyn, respectively, have cysteines at positions 3 and 6 replaced by serines. In the S_3C-Src and S_6C-Src mutants serines at positions 3 and 6, respectively, are replaced by cysteines. In the $G\alpha_o$(10)Fyn, $G\alpha_s$(10)Fyn, and GAP43(10)Fyn chimeric constructs (see Materials and Methods), the first 10 amino acids of Fyn have been replaced with the corresponding sequences of human $G\alpha_o$, $G\alpha_s$ (23), or GAP43 (22).

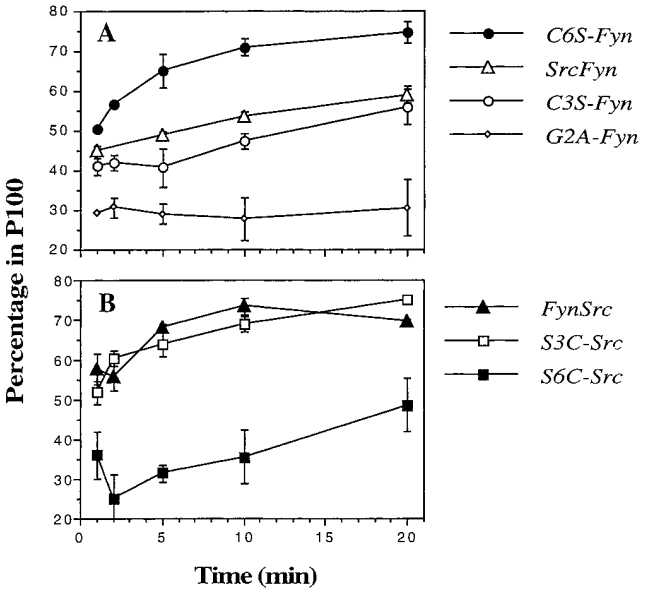

Figure 6. Membrane binding of newly synthesized Fyn or Src chimeric or mutant constructs. COS-1 cells were transfected with chimeric constructs and mutants of Fyn (see Table I). Transfected cells were radiolabeled and fractionated as described in the legend to Fig. 1. Quantitation was performed by phosphorimaging, after exposure of the gels for 2–5 d.

anchoring of newly synthesized Fyn (Fig. 6 *A*), very similar to v-Src (Figs. 1, 2, and 5). Myristoylation was a prerequisite for membrane anchoring, as evidenced by the consistently lower amounts (~30%) of the nonmyristoylated G_2A-Fyn mutant in the membrane fractions (Fig. 6 *A*).

Next, a series of point mutations were used, containing cysteine to serine replacements and vice versa, to eliminate or introduce palmitoylation sites (1). Analysis of C_3S-Fyn and C_6S-Fyn mutants (Table I) showed that rapid membrane targeting of newly synthesized Fyn was selectively abolished by mutation of the cysteine at position-3, but not at position-6 (Fig. 6 *A*). The kinetics of membrane association of C_3S-Fyn (Fig. 6 *A*) were similar to v-Src (Fig. 2 *B*) because a significant amount of newly synthesized protein was found in the soluble fraction, shifting slowly to the membrane fractions. Newly synthesized C_6S-Fyn (Fig. 6 *A*), however, exhibited membrane binding kinetics indistinguishable from that of wt Fyn (Fig. 2 *A*). C_3S-C_6S-Fyn, the construct containing cysteine to serine replacements at both positions 3 and 6 (Table I), behaved in a manner identical to C_3S-Fyn (not shown) confirming the observation that cysteine-3 is essential for rapid membrane targeting.

A parallel set of experiments was performed with potential "gain of function" mutations in Src, in which serines at positions-3 or -6 were replaced by cysteines (1). Introduction of a cysteine residue at position-3 selectively conferred rapid membrane binding to Src; radiolabeled S_3C-Src protein shifted rapidly (<5 min) to the P100 fractions, very similar to the Fyn(14)Src construct (Fig. 6 *B*). However, biosynthetic S_6C-Src (Fig. 6 *B*) displayed the same membrane binding kinetics as v-Src (Fig. 2 *B*). We have previously established that S_3C-Src, but not S_6C-Src, is palmitoylated in COS-1 cells (1). We conclude that the presence of a palmitoylated cysteine at position-3 in the N-myristoylated Src family members is necessary and sufficient for rapid membrane targeting.

Acylation and Membrane Binding of $G\alpha_o$-, $G\alpha_s$-, and GAP43-Fyn Chimeras

Three additional chimeric Fyn constructs were designed in order to independently evaluate the roles of myristate, palmitate, and the surrounding amino acid sequence in rapid membrane binding. The first 10 amino acids of Fyn were replaced with those of other palmitoylated proteins ($G\alpha_o$, $G\alpha_s$, or GAP43), providing Fyn chimeras (Table I) with specific variations on the NH_2-terminal Met-Gly-Cys sequence involved in myristoylation and palmitoylation of Src family proteins (1, 4). The NH_2-terminal sequence of $G\alpha_o$(10)-Fyn contains Met-Gly-Cys and is expected to be dually acylated with myristate and palmitate. The $G\alpha_s$(10)-Fyn chimeric protein also contains the Met-Gly-Cys sequence, as well as an asparagine residue at position 6 (Table I), which precludes N-myristoylation (20). GAP43 (10)-Fyn does not encode an N-myristoylation site, as it contains a leucine at position 2, but it has two palmitoylation sites in the cysteines at positions 3 and 4 (30).

COS-1 cells were transfected with the cDNAs for $G\alpha_o$(10)-Fyn, $G\alpha_s$(10)-Fyn, and GAP43(10)-Fyn, and cells were labeled with either [^{35}S]methionine, 13-[^{125}I]iodotridecanoic acid (IC13), an iodinated myristate analogue (36) or 16-[^{125}I]iodohexadecanoic acid (IC16), and an iodinated palmitate analogue (36). Cells were lysed, immunoprecipitated with anti-Fyn antibody, and analyzed by SDS-PAGE and autoradiography. The labeling patterns for wt Fyn and the $G\alpha_o$(10)-Fyn, $G\alpha_s$(10)-Fyn, and GAP43(10)-Fyn contructs are depicted in Fig. 7. All constructs were expressed to similar levels (Fig. 7, *top row*). In agreement with earlier observations (1), Fyn was found to incorporate both the labeled IC13 and IC16 analogues. $G\alpha_o$(10)-Fyn also incorporated both analogues, although the IC16 incorporation was slightly lower (Fig. 7), likely reflecting the presence of

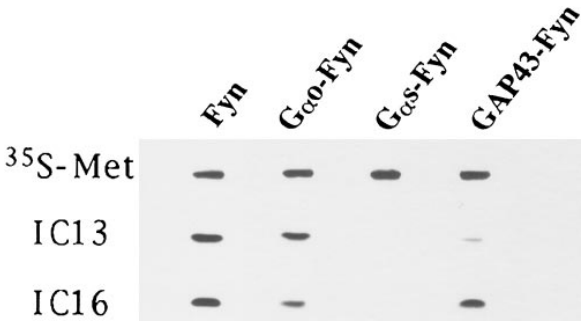

Figure 7. Fatty acylation of $G\alpha_o$(10)-Fyn, $G\alpha_s$(10)-Fyn, and GAP43(10)-Fyn chimeras. COS-1 cells, transfected with Fyn, $G\alpha_o$(10)-Fyn, $G\alpha_s$(10)-Fyn, and GAP43(10)-Fyn chimeric constructs (see Materials and Methods and Table I) were labeled with either [^{35}S]methionine (*top row*), 13-[^{125}I]iodotridecanoic acid (*middle row*), or 16-[^{125}I]iodohexadecanoic acid (*lower row*) as described in the Materials and Methods section. Cell lysates were immunoprecipitated with anti-fyn antibody and analyzed by SDS-PAGE and autoradiography. Strips corresponding to the region of the gel containing $p59^{fyn}$ are shown. No other radiolabeled proteins were apparent on the gel.

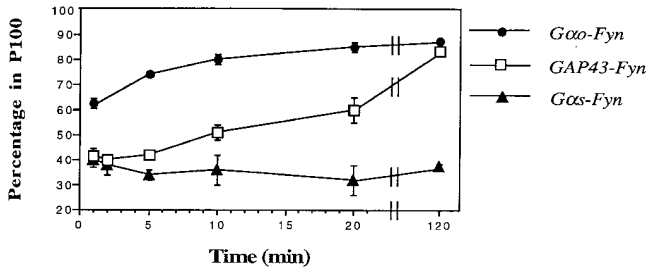

Figure 8. Membrane binding of newly synthesized $G\alpha_o(10)$-Fyn, $G\alpha_s(10)$-Fyn, and GAP43(10)-Fyn chimeras. COS-1 cells were transfected with chimeric constructs (see Table I) and radiolabeled, homogenized, and fractionated as described in the legend under Fig. 1. Quantitation was performed by phosphorimaging, after exposure to the gels for 2–5 d. Numbers are the mean of two experiments.

only one cysteine residue in the NH_2-terminal region (Table I). $G\alpha_s(10)$-Fyn did not incorporate IC13 or IC16, even though the protein was expressed at similar levels to the other constructs. This result was surprising since full-length $G\alpha_s$ has been reported to be palmitoylated (8, 28, 35). For GAP43(10)-Fyn, significant incorporation of IC16 was observed, whereas only trace amounts of IC13 were found. Incorporation of minor amounts of IC13 into GAP43(10)-Fyn may be due to a certain degree of nonspecific recognition of fatty acids by the palmitoyl acyltransferase (PAT) activity (3). Conversion of IC13 into other fatty acids followed by incorporation into the protein seems less likely as this was not observed for the $G\alpha_s(10)$-Fyn construct. For all constructs, identical labeling patterns were obtained using [^{3}H]myristate and [^{3}H]palmitate instead of IC13 and IC16 (not shown).

The chimeric Fyn constructs were then tested in the biosynthetic membrane targeting assay (Fig. 8). Transfected COS-1 cells were radiolabeled for 1, 2, 5, 10, 20, and 120 min at 37°C, homogenized, fractionated into S100 and P100 fractions, and analyzed by SDS-PAGE after immunoprecipitation as before. The $G\alpha_o(10)$-Fyn construct, like wt Fyn, became rapidly enriched in the membrane fractions. Nearly 65% of newly synthesized $G\alpha_o(10)$-Fyn was found in the P100 fraction after labeling for 1 min, shifting to 75% in the P100 after 5 min and 90% at steady state after 120 min (Fig. 8). The $G\alpha_s(10)$-Fyn construct, which is neither myristoylated nor palmitoylated (Fig. 7), behaved as the G_2A-Fyn construct (Fig. 6 *A*), remaining 60–70% soluble over the time course of the experiment (Fig. 8). Interestingly, GAP43(10)-Fyn displayed a slow membrane targeting phenotype, very similar to v-Src. After 1, 2, and 5 min the majority was still in the soluble fraction, shifting to 60% membrane bound after 20 min. The major difference between GAP43(10)-Fyn and v-Src was the higher amount of GAP43(10)-Fyn in the P100 fraction at steady state (cf. Figs. 2 *B* and Fig. 8). Thus, although the GAP43 sequence directed incorporation of palmitate and membrane binding at steady state, it was not sufficient to direct rapid biosynthetic membrane anchoring. These observations substantiate the conclusion that rapid membrane targeting of newly synthesized Fyn is exclusively conferred by the combination of NH_2-terminal myristoylation plus palmitoylation.

Newly Synthesized Fyn Colocalizes with the Plasma Membrane

We next assessed the intracellular localization of newly synthesized Fyn by analysis of homogenates on linear density gradients and comparison to marker enzyme activities for the ER, Golgi complex, and the plasma membrane (Fig. 9). For these experiments, NIH-3T3 fibroblasts stably expressing Fyn were used, in combination with iodixanol gradients. The stable 3T3 cells were used because fractionation of subcellular organelles from transiently transfected COS-1 cells was very difficult, likely due to the presence of DEAE-dextrans in the transfection mix. Iodixanol (OptiPrep™) gradients allowed for a significant separation of plasma membrane marker activity from ER and Golgi activities (Fig. 9), which was not accomplished using sucrose density gradients (not shown). Confluent monolayers of NIH-3T3 cells expressing Fyn were radiolabeled with [^{35}S]methionine for 5 min (Fig. 5), followed by homogenization in an isotonic buffer, preparation of a P100 fraction, and centrifugation through continuous Iodixanol (25–2.5% wt/vol OptiPrep™) gradients. Gradients were fractionated from the bottom (*left*) to the top (*right*) and samples were taken for marker enzyme analysis. α-Glucosidase II was measured as a marker for endoplasmic reticulum (*top panel*), α-mannosidase II as a Golgi marker (*middle panel*) and alkaline phosphatase as a plasma membrane marker (*bottom panel*). The distribution of newly synthesized Fyn protein was assayed by immunoprecipitation of each gradient fraction with anti-Fyn antibody, followed by SDS-PAGE and phosphorimager analysis. The data depicted in Fig. 9 show that newly synthesized Fyn was recovered from light membrane fractions at low Iodixanol densities, exactly overlapping with alkaline phosphatase activity, a marker for the plasma membrane. Little colocalization was observed with ER or Golgi (Fig. 9) or denser organelles such as mitochondria and lysosomes (not shown). Identical results were obtained after adjusting P100 fractions to 25% wt/vol Iodixanol and applying them to the bottom of the density gradients before centrifugation (not shown), indicating that the light fraction in Fig. 8 is a genuine membrane fraction with a low buoyant density. In pulse-chase experiments, where Fyn was labeled for 5 min and chased for 2 h, the radiolabeled protein did not shift to a different location in density gradients (not shown). These results imply that newly synthesized Fyn becomes rapidly targeted to a light-density, plasma membrane-enriched fraction of the cell within minutes after its release from the ribosome.

Binding of Newly Synthesized Fyn to Non-ionic Detergent Resistant Fractions Occurs with a Slower Time Course

Previous studies, using assays with non-ionic detergents, have suggested that the Src family members Fyn and Lck interact with subspecialized regions of the plasma membrane, enriched in the caveolar marker protein, caveolin (47). Based on this and other work (42, 43, 48), it was hypothesized that dual acylation with myristate and palmitate provides a targeting signal for localization to caveolae and/or other detergent resistant structures (29). It is not known whether acquisition of detergent insolubility pre-

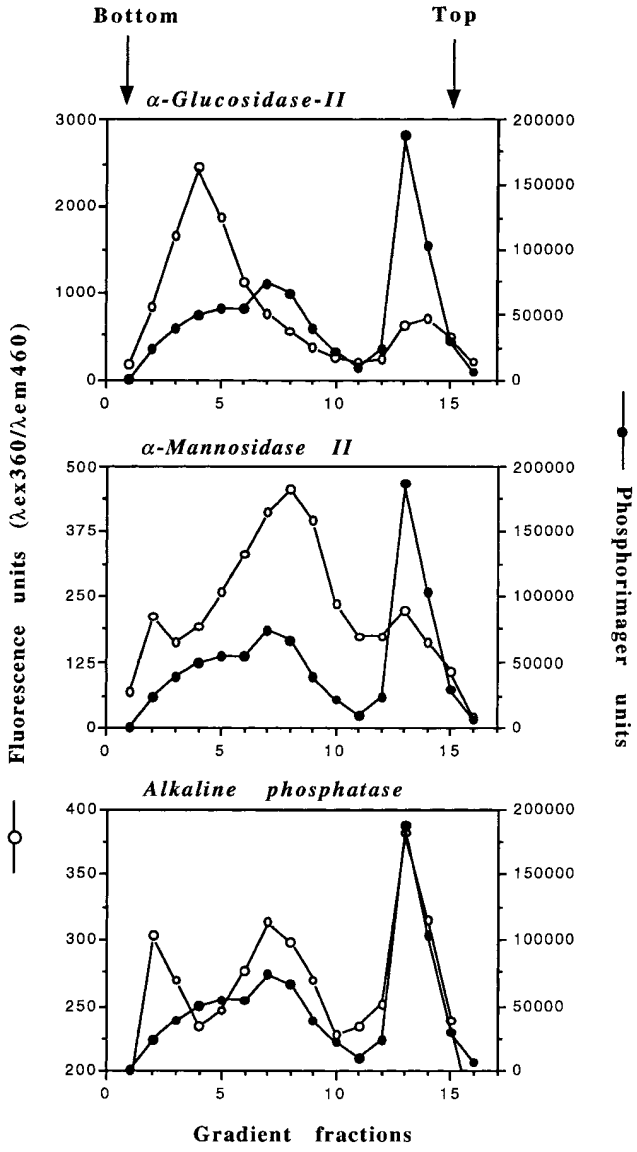

Figure 9. Density gradient analysis of newly synthesized Fyn. Stably transfected NIH-3T3 cells, expressing wt Fyn were radiolabeled for 5 min at 37°C with 500 μCi/ml [^{35}S]methionine as described under Materials and Methods. For each gradient cells from six semi-confluent 100-mm dishes were homogenized in isotonic buffer. After removal of intact cells and nuclei, a P100 fraction was prepared and applied to continuous Iodixanol (25%–2.5% wt/vol OptiPrep™) gradients. Gradients were fractionated from bottom to top (left to right in the figure) and samples were taken for marker enzyme analysis. α-Glucosidase II was measured as a marker for endoplasmic reticulum (*top panel*), α-mannosidase II as a Golgi marker (*middle panel*), and alkaline phosphatase as a plasma membrane marker (*bottom panel*). The distribution of newly synthesized Fyn protein was assayed by subjecting the remainder of each gradient fraction to immunoprecipitation, followed by SDS-PAGE. The intensity of labeled Fyn in each fraction was measured by phosphorimaging, after exposure for 4–6 wk.

cedes or is dependent on membrane binding. Therefore, to study the intracellular fate of biosynthetic Fyn in more detail, we directly compared the kinetics of membrane binding with resistance to 1% Triton X-100 extraction in transfected COS-1 cells. The characteristic rapid membrane binding of Fyn is depicted in Fig. 10, with Fyn becoming entirely membrane-bound within 4 min after the start of biosynthesis. However, at these same early time points (1, 2, and 4 min) the majority (70%) of radiolabeled Fyn was detected in detergent soluble fractions (Fig. 10). The amount of newly synthesized Fyn that was detected in the Triton X-100 resistant fraction at the early timepoints (30%) was similar to that remaining after extraction with 1% Triton X-100 solutions supplemented with deoxycholate and NP-40 (not shown). In addition, this amount is similar to that of the soluble marker protein β-Gal found in the Triton X-100 resistant fraction at steady state, as measured by Western blotting. This indicates that there is approximately a 30% background in the detergent resistant fraction in these experiments. By 6, 8, and 10 min, Fyn became more detergent-resistant, reaching a steady-state level of 55% detergent insolubility after 20 min (Fig. 10). The observed lag-time of 10–20 min between membrane binding of newly synthesized Fyn and enrichment in the detergent resistant fraction strongly suggests that membrane binding of Fyn occurs first, followed by relocalization into a detergent-resistant fraction of the cell.

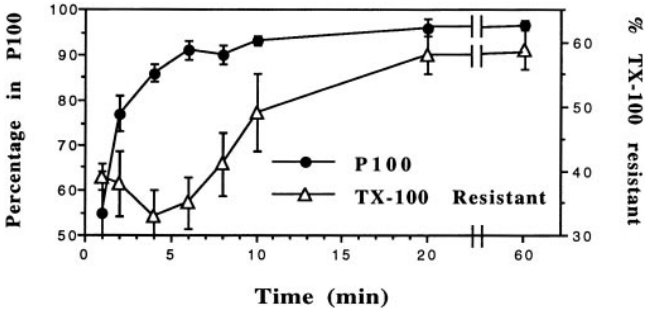

Figure 10. Non-ionic detergent extraction of newly synthesized Fyn. COS-1 cells were transfected with cDNA encoding wild-type Fyn as before. Transfected cells on 60-mm plastic dishes were radiolabeled with 100 μCi/ml [^{35}S]methionine for the indicated times at 37°C, and incubated for 5 min at 4°C with Csk buffer (see Materials and Methods) containing 1% Triton X-100, followed by a wash with Csk buffer. The detergent solutions containing detergent soluble material were pooled and supplemented with lysis buffer. The remaining detergent resistant fractions were scraped from the plates in lysis buffer. Both fractions were clarified and analyzed by immunoprecipitation and SDS-PAGE. In a parallel experiment, cells were fractionated into P100 and S100 fractions as described in the legends to Figs. 1, 2, and 5. Membrane binding and association of newly synthesized Fyn into detergent insoluble complexes was measured by phosphorimaging after exposure for 2–4 d. The graphed values, obtained from four experiments, represent the percentage of total signal recovered in P100 fractions (*closed circles*) or the Triton X-100 resistant fraction (*closed triangles*).

Discussion

Participation of the Src family of nonreceptor tyrosine kinases in signal transduction and cellular transformation requires their binding to cellular membranes. The mechanisms involved in the transport of Src family proteins from their site of synthesis to membranes remain unknown. All

Src family members contain the fatty acid myristate, which is essential, but not sufficient for membrane binding and cell signaling. We aimed to determine whether the recently described dynamic modification of certain Src family members with palmitate is involved in intracellular targeting, using Fyn as a model. Here we demonstrate that the presence of the NH_2-terminal sequence Met-Gly-Cys, the consensus sequence for dual myristoylation and palmitoylation of Src family members, directs rapid membrane targeting of newly synthesized Fyn. The rapidity of membrane binding for Fyn is striking (within 1–4 min after biosynthesis) and stands in distinct contrast to the slower kinetics of membrane binding of nonpalmitoylated Src.

Dual Fatty Acylation Is Required for Rapid Membrane Targeting

Five lines of evidence support the conclusion that the combination of myristate plus palmitate at the NH_2 terminus of Src family proteins directs rapid membrane binding of newly synthesized polypeptides. First, mutation of cysteine-3, a major palmitoylation site in Fyn (1), slows the kinetics as well as the extent of membrane binding of newly synthesized protein (Fig. 6 *A*). Second, introduction of a single cysteine at position 3 in Src converts the membrane binding of Src from "slow" to rapid (Fig. 6 *B*). The S_3C mutation has previously been shown by our laboratory to induce palmitoylation of Src (1). Third, $G\alpha_o$-Fyn, a chimeric protein which is both myristoylated and palmitoylated but contains a different amino acid sequence from position 4-10, displayed rapid binding kinetics identical to wild-type Fyn (Fig. 8). Fourth, although the Met-Gly-Cys sequence is present at the NH_2 terminus of $G\alpha_s$-Fyn (Table I, Fig. 7), only low levels of membrane binding are observed, presumably due to the lack of palmitoylation. Thus, palmitoylation of cysteine-3, rather than the mere presence of cysteine-3, is required for rapid membrane anchoring. Fifth, the GAP43-Fyn chimera, which is palmitoylated but not myristoylated (Fig. 7), exhibits slow membrane binding (Fig. 8), even though >85% of the GAP43-Fyn protein is membrane bound at steady state (Fig. 8). It is noteworthy that the NH_2-terminal sequence of GAP43-Fyn includes three basic amino acid residues, two arginines and a lysine (Table I). Therefore, the two-signal mode for membrane binding of GAP43-Fyn may consist of palmitate plus basic amino acids, analogous to the myristate plus basic amino acid motif of Src.

The data we have presented strongly suggests that Fyn is already dually acylated within 5 min after biosynthesis. N-myristoylation is known to be a cotranslational modification (54), which occurs as the NH_2 terminus of the nascent chain is exposed from the ribosome (10). Protein palmitoylation has been classified as a posttranslational modification, based on the relative resistance of radiolabel incorporation to treatment with protein synthesis inhibitors such as cycloheximide (34). Our data, however, imply that palmitoylation must be occurring relatively soon after protein synthesis has been completed. It is not possible to directly address this issue by pulse-chase analysis with radiolabeled palmitate, since this would not only radiolabel newly synthesized Fyn, but also the pool of existing Fyn undergoing cycles of acylation/deacylation. Instead, we analyzed the effects of protein synthesis inhibitors on palmitoylation of Fyn. Transfected COS-1 cells were pre-treated for 1 h at 37°C with 50 μg/ml cycloheximide and then radiolabeled for 2 h at 37°C with either [^{35}S]methionine, IC13, or IC16 in the presence of cycloheximide. Incorporation of [^{35}S]methionine and IC13 was nearly completely inhibited (>95%), confirming that N-myristoylation is tightly dependent on ongoing protein synthesis. However, levels of IC16 incorporation were also reduced by 65–70%, compared to untreated controls (data not shown). These results confirm that some level of palmitoylation of Fyn can occur in the absence of protein synthesis, but importantly, they also imply that a significant fraction of the radiolabeled palmitate is actually incorporated into newly synthesized Fyn polypeptide.

Our results suggest that palmitoylation is a critical process in determining the intracellular destination of newly synthesized Fyn. Recently, uncatalyzed, acyl-CoA–dependent auto acylation of cysteine-containing lipopeptides or G protein α subunits has been shown to occur in vitro (11, 38). Three observations argue against an uncatalyzed transacylation mechanism to drive rapid membrane binding of Fyn after biosynthesis. First, the exclusive requirement for a cysteine at position-3 but not at position-6 (Fig. 6), and the essential combination with N-myristoylation (Fig. 8) imply that a specific protein-mediated mechanism is involved. Second, the fastest time scale observed for uncatalyzed transacylation in vitro was on the order of tens of minutes, still an order of magnitude slower than the in vivo membrane binding of Fyn. Third, nonenzymatic acylation of Fyn is expected to occur preferentially at intracellular sites with high local concentrations of fatty acids and acyl-CoA-precursors. In intact cells, such a location accessible to soluble Fyn consists of the cytoplasmic membrane aspect of the ER, which is involved in the biosynthesis of phospholipids and ceramides. Newly synthesized Fyn, however, was specifically localized to plasma membrane enriched fraction in density gradients, was entirely absent from the ER fractions at higher densities, and only slightly overlapped with the Golgi complex (Fig. 9). Dunphy et al. (1996) have recently documented the presence of a specific PAT activity in the plasma membrane (12). These observations, therefore, suggest that a protein palmitoyl transferase (PAT) could be the critical component in determining the intracellular destination of newly synthesized Fyn as opposed to random diffusion and trapping of soluble Fyn by non-enzymatic acylation reactions.

Intracellular Trafficking of Fyn

Few studies have examined the biosynthetic trafficking pathways of Src family members. In early work, v-Src was reported to be synthesized on free ribosomes in the cytosol (25). Pulse-chase analysis of Rous sarcoma virus-transformed NRK cells revealed that newly synthesized v-Src shifted from the soluble to the membrane fraction in 5–10 min (26). No study to date has investigated the intracellular trafficking pattern of the dually acylated Src family members (e.g., Fyn, Lck). The data we have presented indicate that Fyn is synthesized on soluble polysomes and is released into the cytosol as a soluble protein. Although the levels of newly synthesized wild-type Fyn in the soluble

fractions were generally low, its cytoplasmic origin was also upheld by the larger cytosolic pools of labeled G_2A-Fyn and C_3S-Fyn mutant protein (Fig. 6 *a*). Rapid association with plasma membranes (or a membrane fraction of similar density) then occurs (Fig. 9), followed by a slower partitioning of the protein into a detergent-resistant matrix (Fig. 10). These results constitute the first demonstration of a unique trafficking pathway for a dually fatty acylated protein, which is characterized by its rapid kinetics, and underscore the importance of fatty acid acylation not only for membrane binding, but also for protein trafficking.

The molecular mechanism behind the novel trafficking pathway that is followed by Fyn between the cytosol and the plasma membrane remains unknown. However, the observation that a single serine to cysteine replacement at position-3 is sufficient to generate rapid membrane targeting of Src (Fig. 6 *b*), suggests that the transport mechanisms used by Fyn and Src are very closely related. Previous studies on Src have shown that newly synthesized polypeptide complexes with two proteins, pp50 and pp90, in the cytosol (5, 33). It has been proposed that the pp50/pp90 complex may deliver newly synthesized v-Src and other proteins to the plasma membrane (7). However, other studies imply that the pp50-pp90 complex functions to stabilize tyrosine kinase activity of the soluble form of v-Src (18, 55). We have also observed proteins of ~50 and ~90 kD that co-immunoprecipitate with newly synthesized Fyn in soluble fractions (not shown). In the absence of specific inhibitors to trap or arrest Fyn in the cytosolic fraction however (see below), the detectable pools of newly synthesized Fyn in soluble fractions were low. As a consequence, the levels of coprecipitating proteins were also low and inconsistent and the significance of these observations therefore remain unclear.

In an attempt to classify the mechanism involved in rapid membrane trafficking of dually acylated proteins, a variety of drugs was used in the membrane binding assay. Inhibitors of vesicular trafficking of newly synthesized transmembrane and secretory proteins from the ER to the plasma membrane (Brefeldin A, monensin, etc.) had no effect on either the kinetics or extent of membrane binding of newly synthesized Fyn (data not shown). In addition, the microtubule-disrupting agents nocodazole and colchicine and the actin stress-fiber depolymerizing drug cytochalasin D did not interfere with rapid membrane binding of Fyn (data not shown). Finally, the general tyrosine-kinase inhibitor genistein and the PI-3 kinase inhibitor wortmannin were also ineffective. The absence of any inhibitory effect of these drugs accentuates the unique nature of this novel membrane trafficking pathway.

Plasma Membrane Localization of Newly Synthesized Fyn

Varying observations have been reported with respect to the steady-state intracellular distribution of Fyn. In human T-lymphocytes, Fyn was mainly associated with centrosomal structures (27) or exclusively in association with the T cell receptor complex at the plasma membrane (15). Immunofluorescence studies in NIH 3T3 cells have localized Fyn to both the plasma membrane and intracellular, perinuclear membranes. We have seen a similar distribution of Fyn overexpressed in COS-1 cells (data not shown). Analysis of newly synthesized Fyn in NIH 3T3 cells on density gradients revealed that Fyn colocalized with plasma membrane marker proteins (Fig. 9). It is known that endosomal membranes can have densities similar to that of the plasma membrane and we can at present not rule out that newly synthesized Fyn rapidly associates with an endosomal fraction first, serving as a shuttle to the plasma membrane. Alternatively, the "slow" kinetics of membrane binding exhibited by Src could reflect routing to an intracellular membrane compartment, and indeed, a significant portion of c-Src is found in the endosomal fraction in fibroblastic cells (21). We are currently applying more detailed fractionation assays in order to resolve these issues.

A number of studies have documented that the myr-Gly-Cys motif serves as a signal for partitioning of dually acylated Src family members to the non-ionic detergent resistant matrix, often referred to as cytoskeleton (17), GEM, DIG, or caveolae (29, 42, 43). These structures are considered to be subspecialized regions of the plasma membrane and/or are found in close proximity to the plasma membrane. We therefore examined the kinetics of association of newly synthesized Fyn with the Triton-resistant fraction and compared them with binding of Fyn to membranes. We observed that membrane binding of newly synthesized Fyn precedes acquisition of detergent resistance by 10–20 min (Fig. 10). From the distinct kinetics it appears clear that dual acylation is a prerequisite, but not a direct targeting signal to the detergent resistant plasma membrane specializations, that may represent cytoskeleton or caveolae. Which cellular event causes the lag between membrane binding and acquisition of detergent insolubility of Fyn remains an open question. It seems unlikely that it reflects lateral diffusion of Fyn, from the site of insertion in the plasma membrane to the detergent-resistant plasma membrane specialization, as lateral diffusion of membrane-bound proteins generally occurs on the order of seconds (13). It is possible that the observed lag-time reflects rapid association of newly synthesized Fyn with an endosomal membrane fraction, as discussed above, followed by translocation to the plasma membrane via a vesicular mechanism and association with the detergent resistant matrix.

Intracellular Targeting of Fyn: A Kinetic "Bilayer Trapping" Model

Our data show a strict correlation between the myr-Gly-Cys motif, dual fatty acylation, and rapid plasma membrane targeting of Fyn. As discussed above, it is still not possible to determine precisely whether palmitoylation precedes membrane binding of Fyn or vice versa. Several lines of evidence suggest that palmitoylation is occurring at the plasma membrane. The palmitoyl acyltransferase activities that palmitoylate Fyn (3) and Gα subunits (12) are membrane bound, enriched in plasma membrane fractions (12), and substrates which are membrane bound are preferentially palmitoylated. For example, we have found that anchoring of a nonmyristoylated Fyn (G_2A-Fyn) to the plasma membrane via a COOH-terminal K-Ras4B tail allows for palmitoylation of cysteine-3 of Fyn (van't Hof, W., R. Louft-Nisenbaum, and M.D. Resh, unpublished

observations). A similar result was obtained for palmitoylation of Gαi subunits in vivo (9). Moreover, in vitro palmitoylation assays require the presence of detergent micelles for efficient palmitoylation (4, 12), implying that the colocalization of enzyme and substrate in a lipid bilayer enhances protein palmitoylation. Finally, Silvius and coworkers have recently shown that lipid-modified, cysteinyl-containing peptides, containing myr-Gly-Cys motifs as found at the NH_2 terminus of Fyn, are preferentially palmitoylated and localized at the plasma membrane (45).

Taken together, the available data presented in this manuscript and previous work suggests the following model. Fyn is synthesized on cytosolic polysomes as a soluble protein and is rapidly and specifically trafficked/shuttled to the plasma membrane, where it is palmitoylated by a plasma membrane bound palmitoyl transferase (12, 45). The dually acylated protein now becomes tightly bound to the plasma membrane bilayer where it remains essentially "trapped" due to the strong hydrophobicity of the dual fatty acid anchor. Our data thus provide experimental support for the kinetic bilayer trapping mechanism recently proposed by Shahinian and Silvius (46). Future studies will be directed towards understanding the functional significance of rapid plasma membrane targeting of newly synthesized Fyn.

We are grateful to Drs. Michele Fuortes and Michael Shiloh in the laboratory of Dr. Carl Nathan at Cornell University Medical College, for expert assistance in using the CytoFluor Fluorescent platereader, and to Dr. Martin Wiedmann (Sloan-Kettering Institute for Cancer Research, New York) for advice on the flotation assay for membrane-bound polyribosomes. We thank Vera Bonilha for assistance with preparing the figures, Raya Louft-Nisenbaum for technical assistance, Melissa Ray for secretarial support and Amy Wolven for critically reading the manuscript.

This work was supported by a grant from the American Cancer Society to M.D. Resh (VM4H). M.D. Resh is an Established Scientist of the American Heart Association. W. van't Hof is a Miriam and Benedict Wolf Cancer Research fellow.

Received for publication 23 December 1996.

References

1. Alland, L., S.M. Peseckis, R.E. Atherton, L. Berthiaume, and M.D. Resh. 1994. Dual myristylation and palmitylation of Src family member p59^{fyn} affects subcellular localization. *J. Biol. Chem.* 269:16701–16705.
2. Appleby, M.W., J.A. Gross, M.P. Cooke, S.D. Levin, X. Qian, and R.M. Perlmutter. 1992. Defective T cell receptor signaling in mice lacking the thymic isoform of p59^{fyn}. *Cell.* 70:751–753.
3. Berthiaume, L., and M.D. Resh. 1995. Biochemical characterization of a palmitoyl acyltransferase activity that palmitoylates myristylated proteins. *J. Biol. Chem.* 270:22399–22405.
4. Berthiaume, L., S.M. Peseckis, and M.D. Resh. 1995. Synthesis and use of Iodo-fatty acid analogs. *Methods Enzymol.* 250:454–466.
5. Brugge, J.S. 1986. Interaction of the Rous sarcoma virus protein pp60^{src} with the cellular proteins pp50 and pp90. *Curr. Topics Microbiol. Immunol.* 123:1–22.
6. Casey, P.J. 1995. Protein lipidation in cell signaling. *Science (Wash. DC).* 268:221–225.
7. Courtneidge, S.A., and J.M. Bishop. 1982. Transit of pp60$^{v\text{-}src}$ to the plasma membrane. *Proc. Natl. Acad. Sci. USA.* 79:7117–7121.
8. Degtyarev, M.Y., A.M. Spiegel, and T.L. Jones. 1993. The G protein alpha s subunit incorporates [^{3}H]palmitic acid and mutation of cysteine-3 prevents this modification. *Biochemistry.* 32:8057–8061.
9. Degtyarev, M.Y., A.M. Spiegel, and T.L.Z. Jones. 1994. Palmitoylation of a G protein α_i subunit requires membrane localization not myristoylation. *J. Biol. Chem.* 269:30989–30903.
10. Deichaite, I., L.P. Casson, H.-P. Ling, and M.D. Resh. 1988. In vitro synthesis of pp60$^{v\text{-}src}$: myristylation in a cell-free system. *Mol. Cell. Biol.* 8: 4295–4301.
11. Duncan, J.A., and A.G. Gilman. 1996. Autoacylation of G protein α subunits. *J. Biol. Chem.* 271:23594–23600.
12. Dunphy, J.T., W.K. Greentree, C.L. Manahan, and M.E. Linder. 1996. G-protein palmitoyltransferase activity is enriched in plasma membranes. *J. Biol. Chem.* 271:7154–7159.
13. Edidin, M. 1991. Translational diffusion of membrane proteins. *In* The Structure of Biological Membranes. P. Yeagle, editor. CRC Press Inc., Boca Raton, FL. 539–572.
14. Franzen, P., P. ten Dijke, H. Ichijo, H. Yamashita, P. Schulz, C.-H. Heldin, and K. Miyazono. 1993. Cloning of a TGFβ type I receptor that forms a heteromeric complex with the TGFβ type II receptor. *Cell.* 75:681–692.
15. Gassmann, M., M. Guttinger, K.E. Amrein, and P. Burn. 1992. Protein tyrosine kinase p59^{fyn} is associated with the T cell receptor-CD3 complex in functional human lymphocytes. *Eur. J. Immunol.* 22:283–286.
16. Glomset, J.A., and C.C. Farnsworth. 1994. Role of protein modification reactions in programming interactions between Ras-related GTP-ases and cell membranes. *Annu. Rev. Cell Biol.* 10:181–205.
17. Hamaguchi, M., and H. Hanafusa. 1987. Association of p60^{src} with Triton X-100-resistant cellular structure correlates with morphological transformation. *Proc. Natl. Acad. Sci. USA.* 84:2313–2316.
18. Hartson, S.D., and R.L. Matts. 1994. Association of Hsp90 with cellular Src-family kinases in a cell-free system correlates with altered kinase structure and function. *Biochemistry.* 33:8912–8920.
19. James, G., and E.N. Olson. 1990. Fatty acylated proteins as components of intracellular signaling pathways. *Biochemistry.* 29:2623–2634.
20. Johnson, D.R., R.S. Bhatnagar, L.J. Knoll, and J.I. Gordon. 1994. Genetic and biochemical studies of protein N-myristoylation. *Annu. Rev. Biochem.* 63:869–914.
21. Kaplan, K.B., J.R. Swedlow, H.E. Varmus, and D.O. Morgan. 1992. Association of p60$^{c\text{-}src}$ with endosomal membranes in mammalian fibroblasts. *J. Cell Biol.* 118:321–333.
22. Kosik, K.S., L.D. Orecchio, G.A. Bruns, L.I. Benowitz, G.P. MacDonald, D.R. Cox, and R.L. Neve. 1988. Human GAP-43: its deduced amino acid sequence and chromosomal localization in mouse and human. *Neuron.* 1: 127–132.
23. Kozasa, T., H. Itoh, T. Tsukamoto, and Y. Kaziro. 1988. Isolation and characterization of the human Gs alpha gene. *Proc. Natl. Acad. Sci. USA.* 85: 2081–2085.
24. Lauring, B., H. Sakai, G. Kreibich, and M. Wiedmann. 1995. Nascent polypeptide-associated complex protein prevents mistargeting of nascent chains to the endoplasmic reticulum. *Proc. Natl. Acad. Sci. USA.* 92: 5411–5414.
25. Lee, J.S., H.E. Varmus, and J.M. Bishop. 1979. Virus-specific messenger RNAs in permissive cells infected by avian sarcoma virus. *J. Biol. Chem.* 254:8015–8022.
26. Levinson, A.D., S.A. Courtneidge, and J.M. Bishop. 1981. Structural and functional domains of the Rous sarcoma virus transforming protein (pp60^{src}). *Proc. Natl. Acad. Sci. USA.* 78:1624–1628.
27. Ley, S.C., M. Marsh, C.R. Bebbington, K. Proudfoot, and P. Jordan. 1994. Distinct intracellular localization of Lck and Fyn protein tyrosine kinases in human T-lymphocytes. *J. Cell Biol.* 125:639–649.
28. Linder, M.E., P. Middleton, J.R. Hepler, R. Taussig, A.G. Gilman, and S.M. Mumby. 1993. Lipid modifications of G proteins: alpha subunits are palmitoylated. *Proc. Natl. Acad. Sci. USA.* 90:3675–3679.
29. Lisanti, M.P., P.E. Scherer, Z.L. Tang, and M. Sargiacomo. 1994. Caveolae, caveolin and caveolin-rich membrane domains: a signalling hypothesis. *Trends Cell Biol.* 4:231–235.
30. Liu, Y., D.A. Fisher, and D.R. Storm. 1993. Analysis of the palmitoylation and membrane targeting domain of neuromodulin (GAP43) by site-specific mutagenesis. *Biochemistry.* 32:10714–10719.
31. Lowy, D.R., and B.M. Willumsen. 1993. Function and regulation of Ras. *Annu. Rev. Biochem.* 62:851–891.
32. McLaughlin, S., and A. Aderem. 1995. The myristoyl-electrostatic switch: a modulator of reversible protein-membrane interactions. *TIBS.* 20:272–276.
33. Oppermann, H., A.D. Levinson, L. Levintow, H.E. Varmus, J.M. Bishop, and S. Kawai. 1981. Two cellular proteins that immunoprecipitate with the transforming protein of Rous sarcoma virus. *Virology.* 113:736–751.
34. Paige, L.A., M.J.S. Nadler, M.L. Harrison, J.M. Cassady, and R.L. Geahlen. 1993. Reversible palmitoylation of the protein-tyrosine kinase p56^{lck}. *J. Biol. Chem.* 268:8669–8674.
35. Parenti, M., M.A. Vigano, C.M. Newman, G. Milligan, and A.I. Magee. 1993. A novel N-terminal motif for palmitoylation of G-protein alpha subunits. *Biochem. J.* 291:349–353.
36. Peseckis, S.M., I. Deichaite, and M.D. Resh. 1993. Iodinated fatty acids as probes for myristate processing and function. Incorporation into pp60$^{v\text{-}src}$. *J. Biol. Chem.* 268:5107–5114.
37. Picard, D., and K. Yamamoto. 1987. Two signals mediate hormone-dependent nuclear localization of the glucocorticoid receptor. *EMBO (Eur. Mol. Biol. Organ.) J.* 6:3333–3340.
38. Quesnel, S., and J. R. Silvius. 1994. Cysteine-containing peptide sequences exhibit facile uncatalyzed transacylation and acyl-CoA-dependent acylation at the lipid bilayer interface. *Biochemistry.* 33:13340–13348.
39. Resh, M.D. 1993. Interaction of tyrosine kinase oncoproteins with cellular membranes. *Biochim. Biophys. Acta.* 1155:307–322.
40. Resh, M.D. 1994. Myristylation and palmitylation of Src family members: the fats of the matter. *Cell.* 76:422–413.

41. Resh, M.D. 1996. Regulation of cellular signaling by fatty acid acylation and prenylation of signal transduction proteins. *Cell Signaling.* 8:403–412.
42. Robbins, S.M., N.A. Quintrell, and J.M. Bishop. 1995. Myristoylation and differential palmitoylation of the HCK protein-tyrosine kinases govern their attachment to membranes and association with caveolae. *Mol. Cell. Biol.* 15:3507–3515.
43. Rodgers, W., B. Crise, and J.K. Rose. 1994. Signals determining protein tyrosine kinase and glycosyl-phosphatidylinositol-anchored protein targeting to a glycolipid-enriched membrane fraction. *Mol. Cell. Biol.* 14:5384–5391.
44. Rothman, J.E., and L. Orci. 1992. Molecular dissection of the secretory pathway. *Nature (Lond.).* 355:409–415.
45. Schroeder, H., R. Leventis, S. Shahinian, P.A. Walton, and J.R. Silvius. 1996. Lipid-modified, cysteinyl-containing peptides of diverse structures are efficiently S-acylated at the plasma membrane of mammalian cells. *J. Cell Biol.* 134:647–660.
46. Shahinian, S., and J. R. Silvius. 1995. Doubly-lipid-modified protein sequence motifs exhibit long-lived anchorage to lipid bilayer membranes. *Biochemistry.* 34:3813–3822.
47. Shenoy-Scaria, A.M., D.J. Dietzen, J. Kwong, D.C. Link, and D.M. Lublin. 1994. Cysteine 3 of Src family protein tyrosine kinases determines palmitoylation and localization in caveolae. *J. Cell Biol.* 126:353–363.
48. Shenoy-Scaria, A.M., L.K.T. Gauen, J. Kwong, A.S. Shaw, and D.M. Lublin. 1993. Palmitylation of an amino-terminal cysteine motif of protein tyrosine kinases $p56^{lck}$ and $p59^{fyn}$ mediates interaction with glycosyl-phosphatidylinositol-anchored proteins. *Mol. Cell. Biol.* 13:6385–6392.
49. Sigal, C.T., W. Zhou, C.A. Buser, S. McLaughlin, and M.D. Resh. 1994. Amino-terminal basic residues of Src mediate membrane binding through electrostatic interaction with acidic phospholipids. *Proc. Natl. Acad. Sci. USA.* 91:12253–12257.
50. Silverman, L., and M.D. Resh. 1992. Lysine residues form an integral component of a novel NH_2-terminal membrane targeting motif for myristylated $pp60^{v\text{-}src}$. *J. Cell Biol.* 119:415–422.
51. Towler, D.A., and J.I. Gordon. 1988. The biology and enzymology of eukaryotic protein acylation. *Annu. Rev. Biochem.* 57:69–99.
52. Walter, P., and A.E. Johnson. 1994. Signal sequence recognition and protein targeting to the ER membrane. *Annu. Rev. Cell Biol.* 10:87–119.
53. Weis-Garcia, F., and J. Massagué. 1996. Complementation between kinase-defective and activation-defective TGF-β receptors reveals a novel form of receptor cooperativity essential for signaling. *EMBO (Eur. Mol. Biol. Organ.) J.* 15:276–289.
54. Wilcox, C., J.-S. Hu, and E.N. Olson. 1987. Acylation of proteins with myristic acid occurs cotranslationally. *Science (Wash. DC).* 238:1275–1278.
55. Xu, Y., and S. Lindquist. 1993. Heat-shock protein hsp90 governs the activity of $pp60^{v\text{-}src}$ kinase. *Proc. Natl. Acad. Sci. USA.* 90:7074–7078.
56. Zhang, F.L., and P.J. Casey. 1996. Protein prenylation: molecular mechanisms and functional consequences. *Annu. Rev. Biochem.* 65:241–269.
57. Zhou, W., L.J. Parent, J.W. Wills, and M.D. Resh. 1994. Identification of a membrane binding domain within the amino terminal region of human immunodeficiency virus-1 Gag protein which interacts with acidic phospholipids. *J. Virol.* 68:2556–2569.